Iterative peptide synthesis in membrane cascades: untangling operational decisions

Wenqian Chen [a], Mahdi Sharifzadeh [a,b], Nilay Shah [a], Andrew G. Livingston [a]

[a] Department of Chemical Engineering, Imperial College London, South Kensington Campus, London SW7 2AZ, United Kingdom
[b] Department of Electronic and Electrical Engineering, University College London, WC1E 7JE, United Kingdom

Abstract

Membrane enhanced peptide synthesis (MEPS) combines liquid-phase synthesis with membrane filtration, avoiding time-consuming separation steps such as precipitation and drying. Although performing MEPS in a multi-stage cascade is advantageous over a single-stage configuration in terms of overall yield, this is offset by the complex combination of operational variables such as the diavolume and recycle ratio in each diafiltration process. This research aims to tackle this problem using dynamic process simulation. The results suggest that the two-stage membrane cascade improves the overall yield of MEPS significantly from 72.2% to 95.3%, although more washing is required to remove impurities as the second-stage membrane retains impurities together with the anchored peptide. This clearly indicates a link between process configuration and operation. While the case study is based on the comparison of single-stage and two-stage MEPS, the results are transferable to other biopolymers such as oligonucleotides, and more complex system configurations (e.g. three-stage MEPS).

Keywords

Membrane enhanced peptide synthesis, biopolymer, membrane cascade, dynamic process model.

Nomenclature

A	membrane area (m^2)
B	membrane permeance ($m \cdot s^{-1} \cdot bar^{-1}$)
c	concentration ($mol \cdot m^{-3}$)
F	volumetric flow rate ($m^3 \cdot s^{-1}$)
k	reaction constant (unit is case-dependent)
n	molar quantity (mol)
P	gauge pressure (barg)
ΔP	transmembrane pressure difference (bar)
R	rejection (dimensionless)
t	time (s)
V	volume (m^{-3})
V_{dia}	diavolume (dimensionless)

Abbreviation

AA	amino acid
CSTR	continuous stirred-tank reactor
MEPS	membrane enhanced peptide synthesis
PFR	plug flow reactor
SPPS	solid phase peptide synthesis

Subscript

1	stage 1
2	stage 2
i	integer (starting from 1)
j	integer (starting from 1)
k	integer (starting from 1)
N	integer (user defined)
P	anchored peptide
S	error sequence

1. Introduction

Biopolymers such as peptides and oligonucleotides have specific biological functions that originate from their unique monomer sequences. The chemical synthesis of these biopolymers is iterative, involving stepwise addition of monomers to a growing polymer chain, followed by post-reaction purification (Lutz et al., 2013; Rogers and Long, 2003).

There are two main challenges for the precise control of polymer sequence. Firstly, the chemistry should ensure each reaction proceeds to completion without side reactions. In the context of peptide, this goal can be achieved with the Fmoc chemistry from conventional solid phase peptide synthesis (SPPS) for most peptides (Albericio, 2000; Behrendt et al., 2016; Coin et al., 2007; El-Faham and Albericio, 2011). Secondly, the purification step should ensure the complete removal of excess monomers as well as excess reagents and by-products in order to avoid side reactions in the subsequent steps due to carry-over (Chen et al., 2017).

Membrane enhanced peptide synthesis (MEPS) addresses this purification challenge with the membrane process, which has been used for various applications (Cseri et al., 2016; Dong et al., 2017; Fodi et al., 2017; Gao et al., 2017; Shi et al., 2016). The valuable peptide is grown attached to a soluble anchor (Castro et al., 2017; Gravert and Janda, 1997) in the liquid phase with standard Fmoc chemistry. The soluble anchor aids the retention of the peptide by the membrane during diafiltration (Figure 1) (So et al., 2010a, 2010b). As a result, the excess monomers, reagents and by-products permeate through the membrane, while the anchored peptide remains in the system for further elongation. It was demonstrated previously that this process (and a similar approach for oligonucleotides) can achieve high yield and purity, while offering scalability and ease of monitoring of the impurity level (Castro et al., 2017; Kim et al., 2016; So et al., 2010a, 2010b; Székely et al., 2014).

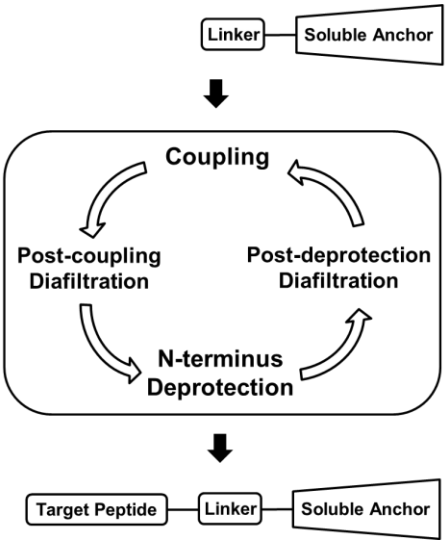

Figure 1. Membrane enhanced peptide synthesis (MEPS).

The configuration of the membrane system and the operation of the diafiltration are important for the purification of anchored peptide in MEPS. It was shown previously that diafiltration in a single-stage nanofiltration system can lead to significant yield loss in order to achieve high purity. This can be overcome by operating diafiltration in a two-stage membrane cascade, where the anchored peptide permeating through the first-stage membrane is recovered by the second-stage membrane (Kim et al., 2014, 2013).

Membrane cascades have been widely studied for applications such as desalination, water purification and the fractionation of solutes in mixture (Abatemarco et al., 1999; Caus et al., 2009; Ebara et al., 1978; Mayani et al., 2009; Mellal et al., 2007). The design and operation of membrane cascades can be complex due to the many combinations of design and operation variables. As a result, computer-aided process simulation and optimisation are useful tools and design aids (Buabeng-Baidoo and Majozi, 2015; Cheang and Zydney, 2004; Fikar et al., 2010; Ghosh, 2003; Khor et al., 2011; Li, 2012; Lightfoot, 2005; Ng et al., 2007; Overdevest et al., 2002; Schaepertoens et al., 2016; van der Meer et al., 1996; van Reis and Saksena, 1997; Voros et al., 1997).

Membrane-enhanced synthesis of biopolymers in membrane cascades is an interesting area of research due to the semi-batch and iterative nature of the process (vs continuous operation for most of the existing studies), as well as the interesting interplay between reaction and purification. However, its complexity in terms of design and operation is a barrier for its adoption in manufacturing in general.

This study presents the advantages of operating an iterative peptide synthesis in a two-stage membrane cascade through process simulations. A dynamic process model was first developed and validated with the experimental data of MEPS in a single-stage system. The process model was then extended to MEPS in a two-stage membrane cascade and an operational variable analysis was performed to show how operating in a two-stage membrane cascade could improve the overall yield of the process.

2. Materials and methods

The materials and experimental procedures for the MEPS of a model hexapeptide (sequence: Pyr-Ser(Bzl)-Ala-Phe-Asp-Leu-NH_2 (Figure S1 in supplementary information)) were reported previously (Chen, 2015; Chen et al., 2017). The anchor used in this experiment was 2,4-didocosyloxybenzalcohol with Rink functionality (Figure S2 in supplementary information). The experimental data were used for the development and validation of the process model of MEPS.

3. Dynamic process simulation

A dynamic process model of MEPS in a single-stage system was developed with an equation-oriented simulation platform, gPROMS, based on the experimental data reported previously (Chen et al., 2017). The MEPS process was performed iteratively in batch mode (according to the number of amino acids in the sequence), where cycles of reaction and filtration were performed in the same single-stage system that comprises mainly a membrane circuit and a feed tank. The operation time for each reaction and diafiltration is an important process variable that determines the purity and yield of each intermediate product at the end of the reaction or diafiltration. The model was validated with the experimental results for overall yield and purity of anchored peptide. The validated model was then extended to MEPS in a two-stage membrane cascade. All the simulation inputs can be found in the supplementary information section. In addition, the simulation file can be downloaded in the supplementary information section.

3.1 Single-stage membrane system: process description

The single-stage membrane system has the simplest design of its kind, comprising nine units (Figure 2). The membrane circuit consists of five units: a circulation pump, three pipes and a membrane unit. The feed pump pushes the liquid from the feed tank into the membrane circuit, whereas the circulation pump ensures the direction of flow as well as good mixing within the membrane circuit. The backpressure valve sets the operating pressure of the membrane circuit by releasing some liquid into

the feed tank (i.e. the recycle), when the feed pump pushes liquid into the membrane circuit and causes the pressure to go beyond the set value. The waste tank collects the permeate from the membrane unit as waste. This simple configuration can be easily turned into a multi-stage system by adding more membrane circuits in sequence.

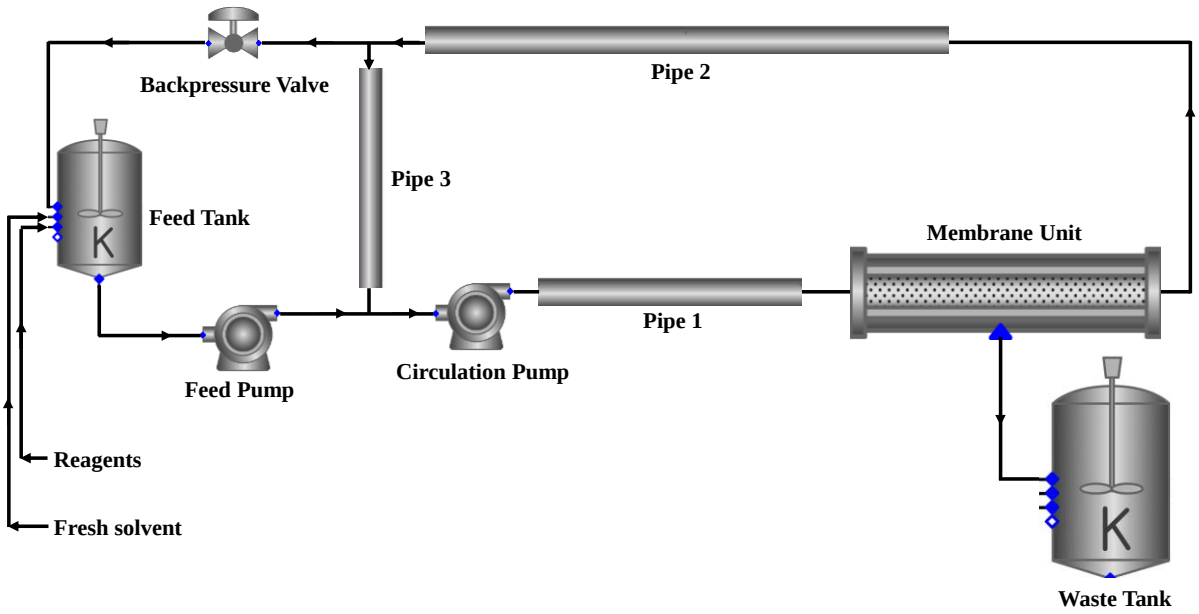

Figure 2. Single-stage membrane system in gPROMS.

3.2 Mass balance during reactions

The current dynamic model calculates the mass balance of each chemical component during reactions and diafiltrations in all unit operations (i.e. the tanks, valves, pumps, pipes and membrane unit in Figure 1). All reactions are modelled dynamically throughout the process, even during diafiltrations where the reactant concentrations drop significantly. This allows the current model to capture the complex nature of the transition between reactions and diafiltrations.

For the addition of each amino acid onto the peptide chain, the anchored peptide first undergoes N-terminus deprotection with piperidine and then coupling with the activated amino acid (Figure 1). The total number of reactions for synthesising a peptide sequence with N amino acids and Fmoc-protection at the N-terminus is therefore equal to 2 N – 1. In this study, the synthesis of the hexapeptide (i.e. N = 6) involves 11 reactions (i.e. 5 deprotections and 6 couplings).

The key components for the peptide synthesis include piperidine, amino acids and anchored peptides (i.e. the target product of reaction (i), where i = 1, 2, 3 … 2 N – 1). In the mass balance, all the amino

acids and anchored peptides are assigned specific numbers (i.e. $AA(i)$ where i = 1, 2, 3 … N and $P(j)$ where j = 1, 2, 3 … 2 N – 1). This allows the identification of individual components for analysis purposes.

For example, in the MEPS of hexapeptide in this study, AA(1) and AA(6) are the first and last amino acids to participate in the couplings, whereas P(1) and P(11) refer to Fmoc-AA(1)-Anchor and Fmoc-AA(6)-AA(5)-AA(4)-AA(3)-AA(2)-AA(1)-Anchor respectively.

For illustration, the mass balance of piperidine, amino acids and anchored peptide intermediates during reactions in a continuous stirred-tank reactor (CSTR) is explained in detail. These calculations are adopted for the different units in the membrane system according to their configurations (i.e. CSTR or plug flow reactor (PFR)). More information can be found in the supplementary information section.

3.2.1 Mass balance for piperidine

Piperidine is not consumed in all reactions. As a result, the rate of accumulation must be equal to the difference between the rates of piperidine entering and leaving the CSTR as shown in Equation 1, where V_{CSTR} is the tank volume (m^3), $c_{inlet,piperidine}$, $c_{outlet,piperidine}$ and $c_{CSTR,piperidine}$ are the concentrations of piperidine at the inlet, outlet and inside the tank ($mol \cdot m^{-3}$), F_{inlet} and F_{outlet} are the volumetric flow rates at the inlet and outlet of the tank ($m^3 \cdot s^{-1}$).

$$V_{CSTR} \times \frac{dc_{CSTR,piperidine}}{dt} = F_{inlet} \times c_{inlet,piperidine} - F_{outlet} \times c_{outlet,piperidine} \quad (1)$$

3.2.2 Reaction network of amino acids and anchored peptides

As reported previously (Chen et al., 2017), a complex reaction network of amino acids and anchored peptides exits due to the formation of error sequences when a deprotected anchored peptide reacts with the residual amino acids from previous couplings. For example, in the second coupling (i.e. n = 2), H_2N-AA(1)-Anchor can react with residual AA(1) to form the error sequence AA(1)-AA(1)-Anchor. The current process model includes the formation of error sequences, so that the extent of removal of amino acids during diafiltration has a direct impact on the final purity of the anchored peptide.

3.2.3 Mass balance for amino acids

In each coupling, a specific amino acid is added into the system for reacting with the deprotected N-terminus of the anchored peptide. However, this amino acid can undergo two more side reactions in the

following steps. The first is the side reaction with piperidine during deprotection, as it was observed experimentally that piperidine consumes activated amino acids in this study. The second side reaction is the formation of error sequence in the following coupling (Chen et al., 2017).

As a result, the mass balance of each amino acid is calculated by Equation 2, where $P(2i-2)$ is the anchored peptide to be coupled with the amino acid $AA(i)$ to give the correct sequence.

$$V_{CSTR} \times \frac{dc_{CSTR,AA(i)}}{dt} = F_{inlet} \times c_{inlet,AA(i)} - F_{outlet} \times c_{outlet,AA(i)} - V_{CSTR} \times k_{coupling} \times c_{CSTR,AA(i)} \times c_{CSTR,P(2i-2)} - V_{CSTR} \times k_{coupling} \times c_{CSTR,AA(i)} \times c_{CSTR,P(2i)} - V_{CSTR} \times k_{side-reaction} \times c_{CSTR,AA(i)} \times c_{CSTR,piperidine} \quad (2)$$

3.2.4 <u>Mass balance for anchored peptides</u>

There are two types of anchored peptides. One has Fmoc-protected N-terminus after coupling and the other is the deprotected form after deprotection. In the mass balance, the anchored peptides are designated as $P(j)$ where j = 1, 2, 3 … 2 N – 1. The Fmoc-protected anchored peptides correspond to $P(j)$ when j is an odd number, whereas the deprotected anchored peptides correspond to $P(j)$ when j is an even number.

Each Fmoc-protected anchored peptide is formed by the prior deprotected anchored peptide during coupling and is then consumed in the deprotection. Therefore, the mass balance for the Fmoc-protected anchored peptide is calculated by Equation 3, where j is an odd number (i.e. 1, 3, 5 …).

$$V_{CSTR} \times \frac{dc_{CSTR,P(j)}}{dt} = F_{inlet} \times c_{inlet,P(j)} - F_{outlet} \times c_{outlet,P(j)} + V_{CSTR} \times k_{coupling} \times c_{CSTR,AA\left(\frac{j+1}{2}\right)} \times c_{CSTR,P(j-1)} - V_{CSTR} \times k_{deprotection} \times c_{CSTR,P(j)} \times c_{CSTR,piperidine} \quad (3)$$

On the other hand, the deprotected anchored peptide is formed during deprotection and is then consumed in the following coupling. In addition, it is also consumed by the side-reaction with residual amino acid from the previous coupling. Therefore, the mass balance for the deprotected anchored peptide is calculated by Equation 4, where j is an even number (i.e. 2, 4, 6 …).

$$V_{CSTR} \times \frac{dc_{CSTR,P(j)}}{dt} = F_{inlet} \times c_{inlet,P(j)} - F_{outlet} \times c_{outlet,P(j)} + V_{CSTR} \times k_{deprotection} \times c_{CSTR,P(j-1)} \times c_{CSTR,piperidine} - V_{CSTR} \times k_{coupling} \times c_{CSTR,AA\left(\frac{j+2}{2}\right)} \times c_{CSTR,P(j)} - V_{CSTR} \times k_{side-reaction} \times c_{CSTR,AA\left(\frac{j}{2}\right)} \times c_{CSTR,P(j)} \quad (4)$$

3.2.5 Mass balance for error sequences

The error sequences are formed by the side-reaction between residual amino acid and deprotected anchored peptide (Chen et al., 2017). The mass balance of these error sequences can be calculated by Equation 5, where $S(k)$ represents the error sequence and k is 1, 2, 3 … N for synthesising a peptide with N amino acids.

$$V_{CSTR} \times \frac{dc_{CSTR,S(k)}}{dt} = F_{inlet} \times c_{inlet,S(k)} - F_{outlet} \times c_{outlet,S(k)} + V_{CSTR} \times k_{side-reaction} \times c_{CSTR,AA(k)} \times c_{CSTR,P(2k)} \quad (5)$$

3.3 Mass balance during diafiltration

Post-reaction diafiltration is necessary for the removal of all excess reagents (i.e. amino acid and piperidine) through the membrane, which is modelled as two CSTRs connected by a membrane interface (Figure 3(a)). This is based on the assumption that perfect mixing is achieved within both the retentate and permeate compartments due to flow turbulence.

When the two compartments are at the same pressure, there is no liquid flow through the membrane and the liquid flows into the retentate compartment of the membrane through the inlet and then exits through the outlet (retentate) (Figure 3 (b)). In this case, no mass transfer takes place through the membrane.

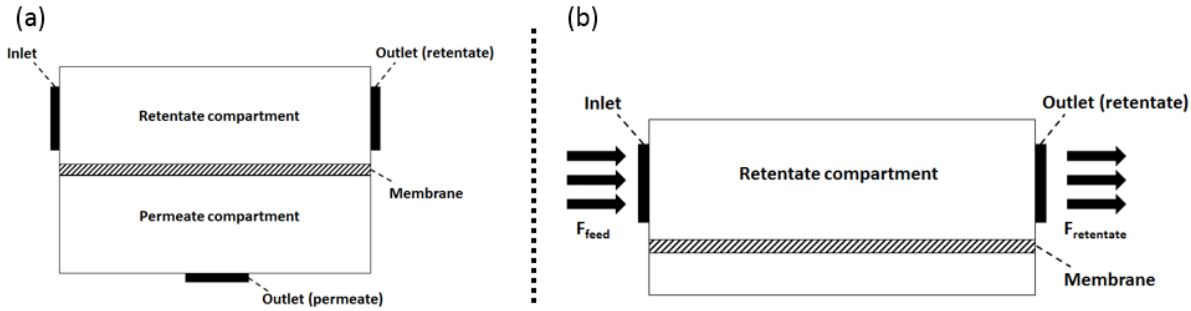

Figure 3. (a) Membrane unit. (b) Liquid flow without cross-membrane pressure difference.

When the retentate compartment has a higher pressure than the permeate compartment, part of the liquid entering from the inlet passes through the membrane and then exits the permeate compartment through the permeate outlet (Figure 4(a)).

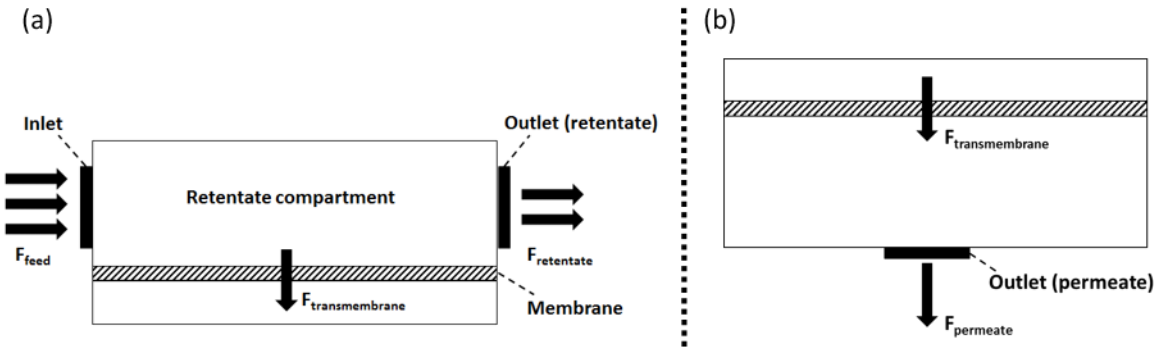

Figure 4. (a) Liquid flow in the retentate compartment with cross-membrane pressure difference. (b) Liquid flow in the permeate compartment with cross-membrane pressure difference.

Assuming perfect mixing, the retentate compartment is modelled after a conventional CSTR, whose general mass balance is described by Equation 6. The transmembrane flow rate, $F_{transmembrane}$ ($m^3 \cdot s^{-1}$), is calculated by Equation 7. The permeance is a physical property of the membrane and can only be changed by using different kind of membrane. The membrane area can be increased by having a bigger module or multiple parallel modules, while the cross-membrane pressure difference (i.e. $\Delta P = P_{retentate} - P_{permeate}$) is an operating variable. For a nanofiltration membrane, the maximum value of cross-membrane pressure difference is normally 40 – 50 bar.

$$V_{retentate} \times \frac{dc_r}{dt} = F_{feed} \times c_{feed} - F_{retentate} \times c_{retentate} - F_{transmembrane} \times c_{transmembrane} + V_{retentate} \times rate(generation) \quad (6)$$

where F_{feed} and $F_{retentate}$ ($m^3 \cdot s^{-1}$) are the volumetric flow rates through the inlet and outlet, $F_{transmembrane}$ ($m^3 \cdot s^{-1}$) is the volumetric flow rate through the membrane, $V_{retentate}$ (m^3) is the volume of the retentate compartment, c_r, c_{feed}, $c_{retentate}$ and $c_{transmembrane}$ ($mol \cdot m^{-3}$) are the concentrations of the compound inside the compartment, at the inlet and outlet, and on the permeate side of the membrane tank respectively.

$$F_{transmembrane} = B \times \mathrm{A} \times \left(P_{retentate} - P_{permeate}\right) \tag{7}$$

where $F_{transmembrane}$ ($m^3 \cdot s^{-1}$) is the volumetric flow rate through the membrane, B ($m \cdot s^{-1} \cdot bar^{-1}$) is the permeance of the membrane, A (m^2) is the membrane area, and $P_{retentate}$ and $P_{permeate}$ (barg) are the gauge pressure of the retentate and permeate compartments respectively.

Similarly, the mass balance in the permeate compartment of the membrane unit (Figure 4(b)) can be calculated by Equation 8, where $F_{transmembrane}$ and $F_{permeate}$ ($m^3 \cdot s^{-1}$) are the volumetric flow rates through the membrane and outlet, $V_{permeate}$ (m^3) is the volume of the permeate compartment, c_p, $c_{transmembrane}$ and $c_{permeate}$ are the concentrations of the compound inside, entering and leaving the compartment. The concentration of the compound entering the permeate compartment is correlated to the concentration at the outlet of the retentate compartment by Equation 9, where R is the rejection of the compound by the membrane.

$$V_{permeate} \times \frac{dc_p}{dt} = F_{transmembrane} \times c_{transmembrane} - F_{permeate} \times c_{permeate} + V_{permeate} \times rate(generation) \tag{8}$$

$$R = 1 - \frac{c_{transmembrane}}{c_{retentate}} \tag{9}$$

3.4 <u>MEPS in two-stage membrane cascade</u>

After the development and validation with experimental data, the process model was extended to the two-stage membrane cascade, which has an additional membrane circuit (Figure 5). The second-stage membrane serves to recover the anchored peptide that permeates through the first-stage membrane and recycle it back to the feed tank. As a result, less anchored peptide leaves the entire membrane system as waste.

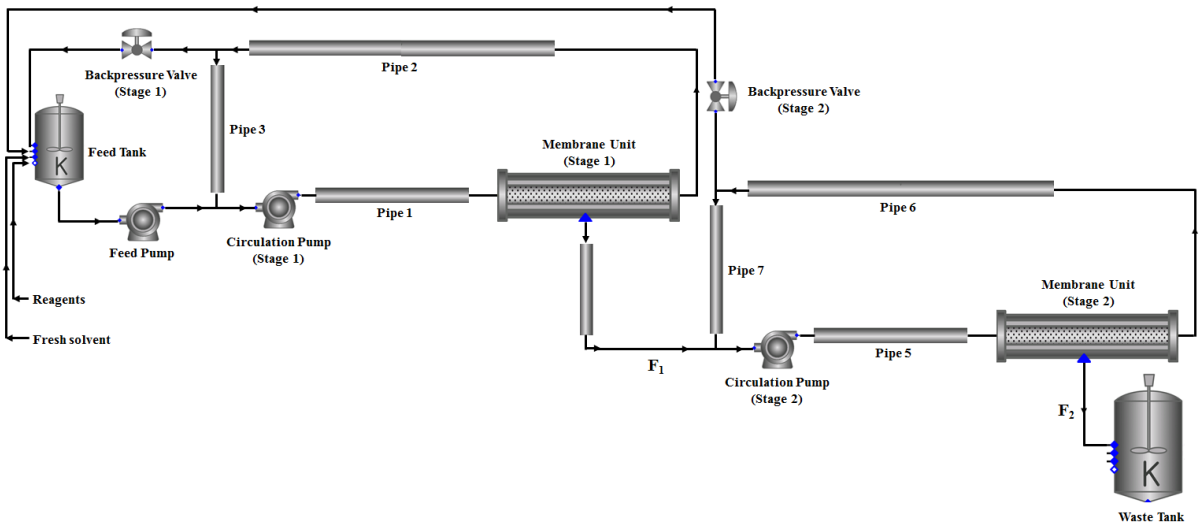

Figure 5. Two-stage membrane cascade in gPROMS.

3.5 Variables for performance analysis

Due to the large number of variables in the process simulation, several consolidating variables were introduced to analyse the process performance, including synthesis scale, yield, purity, conversion, diavolume, extent of removal, recycle ratio and minimum selling price of the anchored peptide.

Since one mole of deprotected peptide forms one mole of extended N-terminus-protected peptide in a coupling and one mole of N-terminus-protected peptide forms one mole of deprotected peptide in a deprotection, the synthesis scale (mol) is defined as the quantity of anchor used in the first coupling ($n_{anchor,initial}$) (mol) (Equation 10).

$$synthesis\ scale = n_{anchor,initial} \tag{10}$$

The yield of anchored peptide ($yield_{P(i)}$) (%) is defined as the quantity of anchored peptide ($n_{P(i)}$) (mol) normalised by the quantity of anchor used in the first coupling ($n_{anchor,initial}$) (mol) (Equation 11).

$$yield_{P(i)} = \frac{n_{P(i)}}{n_{anchor,initial}} \times 100\ \% \tag{11}$$

The purity of anchored peptide ($purity_{P(i)}$) (%) is defined as the quantity of anchored peptide ($n_{P(i)}$) (mol) normalised by the total quantity of chemical components in the system (n_{total}) (mol) including amino acids, piperidine, side products and anchored peptides (Equation 12).

$$purity_{P(i)} = \frac{n_{P(i)}}{n_{total}} \times 100\ \% \tag{12}$$

The conversion of anchored peptide in a reaction (i.e. coupling or deprotection) ($Conversion_{P(i)}$) (%) is defined as the quantity of the resulting anchored peptide ($n_{P(i+1)}$) (mol) normalised by the quantity of the starting anchored peptide ($n_{P(i)}$) (mol) (Equation 13).

$$Conversion_{P(i)} = \frac{n_{P(i+1)}}{n_{P(i)}} \times 100\ \% \tag{13}$$

In constant volume diafiltration, diavolume (V_{dia}) is a dimensionless term for quantifying the total volume of permeate with respect to the system volume (V_{system}) (Equation 14) (Kim et al., 2013).

$$V_{dia} = \frac{A \times B \times \Delta P \times t}{V_{system}} \tag{14}$$

where B (m · s^{-1} · bar^{-1}) is the permeance of the membrane, A (m^2) is the membrane area, ΔP is the cross-membrane pressure difference (bar) as in Equation 7, t (s) is the diafiltration time and V_{system} (m^3) is the system liquid volume.

During constant volume diafiltration, chemical components permeate through the membrane with the solvent. As a result, the extent of removal of a particular chemical component increases with the diavolume. The extent of removal for component i ($Extent\ of\ removal_i$) is defined as the quantity of the chemical component (n_i) (mol) at the end of diafiltration normalised by its quantity at the beginning of the diafiltration ($n_{i,initial}$) (mol) (Equation 15).

$$Extent\ of\ removal_i = \frac{n_i}{n_{i,initial}} \times 100\ \% \tag{15}$$

As pointed out in a previous study, the recycle ratio ($recycle$) (%) is an important higher-order variable in membrane cascade operation (Kim et al., 2013). The recycle ratio ($recycle$) (%) at the second-stage membrane circuit (Figure 5) is defined as the percentage of the volumetric flow through the first-stage membrane (F_1) (m^3 · s^{-1}) (Equation 16) that is recycled back to the feed tank. The recycle ratio is correlated to both design (A_1 and A_2) (m^2) and operating variables (ΔP_1 and ΔP_2) (bar) (Equation 18b). A high recycle ratio (i.e. close to 100%) means most of the volumetric flow through the first-stage membrane is recycled back to the feed tank.

$$F_1 = B_1 \times A_1 \times \Delta P_1 \tag{16}$$

$$F_2 = B_2 \times A_2 \times \Delta P_2 \tag{17}$$

$$recycle = \frac{F_1 - F_2}{F_1} \times 100\ \% = \frac{B_1 \times A_1 \times \Delta P_1 - B_2 \times A_2 \times \Delta P_2}{B_1 \times A_1 \times \Delta P_1} \times 100 \qquad (18a)$$

Since the same type of membrane is used in both stage 1 and 2, $B_1 = B_2$:

$$recycle = \frac{A_1 \times \Delta P_1 - A_2 \times \Delta P_2}{A_1 \times \Delta P_1} \times 100\ \% \qquad (18b)$$

where $recycle$ (%) is the recycle ratio, F_1 and F_2 ($m^3 \cdot s^{-1}$) are the volumetric flow rate through the membranes of stage 1 and 2 respectively (Figure 5), B ($m \cdot s^{-1} \cdot bar^{-1}$) is the permeance, A (m^2) is the membrane area and ΔP (bar) is the cross-membrane pressure difference.

The minimum selling price (Euro $\cdot$ g^{-1}) of the anchored peptide is used to evaluate the economic performance of the process (Equation 19). It includes the amortisation of capital investment, maintenance of equipment, membrane replacement, chemicals, labour and electricity (Sethi and Wiesner, 2000; Suárez et al., 2015). The details of the economic model can be found in Section S6 in the supplementary information as well as the previous literature (Chen, 2015).

$$Minimum\ selling\ price = \frac{(A_C + C_{MC} + C_{MA})}{AP} + \frac{(C_E + C_C + C_L)}{CP} \qquad (19)$$

where A_C(Euro $\cdot$ $year^{-1}$) is the amortisation constituent, C_{MC}(Euro $\cdot$ $year^{-1}$) is the cost of membrane replacement, C_{MA}(Euro $\cdot$ $year^{-1}$) is the cost of maintenance, C_E (Euro $\cdot$ $cycle^{-1}$) is the cost of energy, C_C (Euro $\cdot$ $cycle^{-1}$) is the cost of chemicals, C_L (Euro $\cdot$ $cycle^{-1}$) is the cost of labour, AP ($g \cdot year^{-1}$) is the annual production rate of product and CP ($g \cdot cycle^{-1}$) is the cycle production rate of product.

4. Results and discussions

In this section, the process model of MEPS in a single-stage membrane system was validated with experimental data and then extended to a two-stage membrane cascade. The dynamic quantities of intermediate products (i.e. the growing anchored peptide chain), as well as the overall yield for single-stage and two-stage systems were compared in order to show the advantage of performing MEPS in a two-stage cascade. Operational variable analysis was then performed to show the overall yield can change with operating variables such as the diavolume of post-coupling diafiltration and recycle ratio.

4.1 Validation of process model in single-stage membrane system

The process model enables the dynamic simulation of all couplings, N-terminus deprotection and post-reaction diafiltrations. The simulation inputs for single-stage MEPS are summarised in Section S2 in the supplementary information.

The structural analysis of the gPROMS model shows that there are 711 variables, of which 209 are assigned and the remaining 502 are calculated. The model has 502 equations, of which 180 are ordinary differential equations and 322 are algebraic equations. In order to solve the system of equations, 180 initial conditions are provided. As a result, there are no degrees of freedom. Unlike other software such as MATLAB, it is not necessary to specify the calculation sequence in gPROMS, since it is handled by the software internally as part of the equation-oriented solution approach.

The assumptions for the calculation of mass balance are listed below:

1. Tubes behave as PFRs.
2. Tanks and compartments in membrane units behave as CSTRs.
3. Membrane has constant rejection for each component and constant permeance.
4. The reactions are first-order with respect to each participating reactant.
5. The coupling reactions have the same rate constant.
6. The N-terminus deprotection reactions have the same rate constant.

Assumption 1 and 2 are valid due to the high flow rates within the system. Assumption 3 is valid for ceramic membrane that was used in the current study, but may not be invalid for polymeric membrane during compression. Assumption 4 is valid due to the known chemistry of coupling and N-terminus

deprotection, but should be modified if the reactions follow more complicated pathways. Assumption 5 and 6 are valid for the reactions with short peptides, but could be invalid for longer ones whose properties are more dependent on peptide length.

The process model of MEPS in a single-stage membrane system is validated with the results in Table 1. This table shows that there is a close agreement between the overall yield and purity of the anchored peptide (structure shown in Figure S3 of supplementary information) calculated by the model (72.2 % and 89.1 % respectively) and their corresponding experimental values (71.2 % and 88.1 % respectively).

Table 1. Experimental and modelling results of single-stage MEPS.

	Experimental	**Modelling**
Overall yield* (%)	71.2	72.2
Final purity (%)	88.1	89.1%

*The overall yield was before cleavage and global deprotection (i.e. the peptide was still bound to the anchor).

Figure 6 shows that the current process model accurately captures the dynamic interactions between two consecutive anchored peptides. Except for the anchored peptides with the full sequence, all the other anchored peptides go through three general stages in MEPS:

1. Formation through the coupling reaction
2. Purification by diafiltration
3. Consumption as the next peptide in the sequence is formed

When put together, the rise and fall in the quantity of each anchored peptide over time forms a wave pattern in Figure 6. Each operation (i.e. coupling, N-terminus deprotection, post-coupling diafiltration and post-N-terminus-deprotection) had a fixed processing time based on the experimental values, which are specified in Table S2 and S3 in the supplementary information.

Using Fmoc-AA(1)-Anchor as an example, its quantity increases from zero to the synthesis scale (i.e. 33.6 mmol) in the first coupling, as the anchor reacts with Fmoc-AA(1). In the post-coupling diafiltration, its quantity decreases slightly due to its permeation through the membrane. Its quantity diminishes rapidly in the next deprotection, where it reacts with piperidine to form the next anchored peptide, H_2N-AA(1)-Anchor. The general downward trend of anchored peptide quantities over time was mainly due to the mass loss through the membrane during diafiltrations.

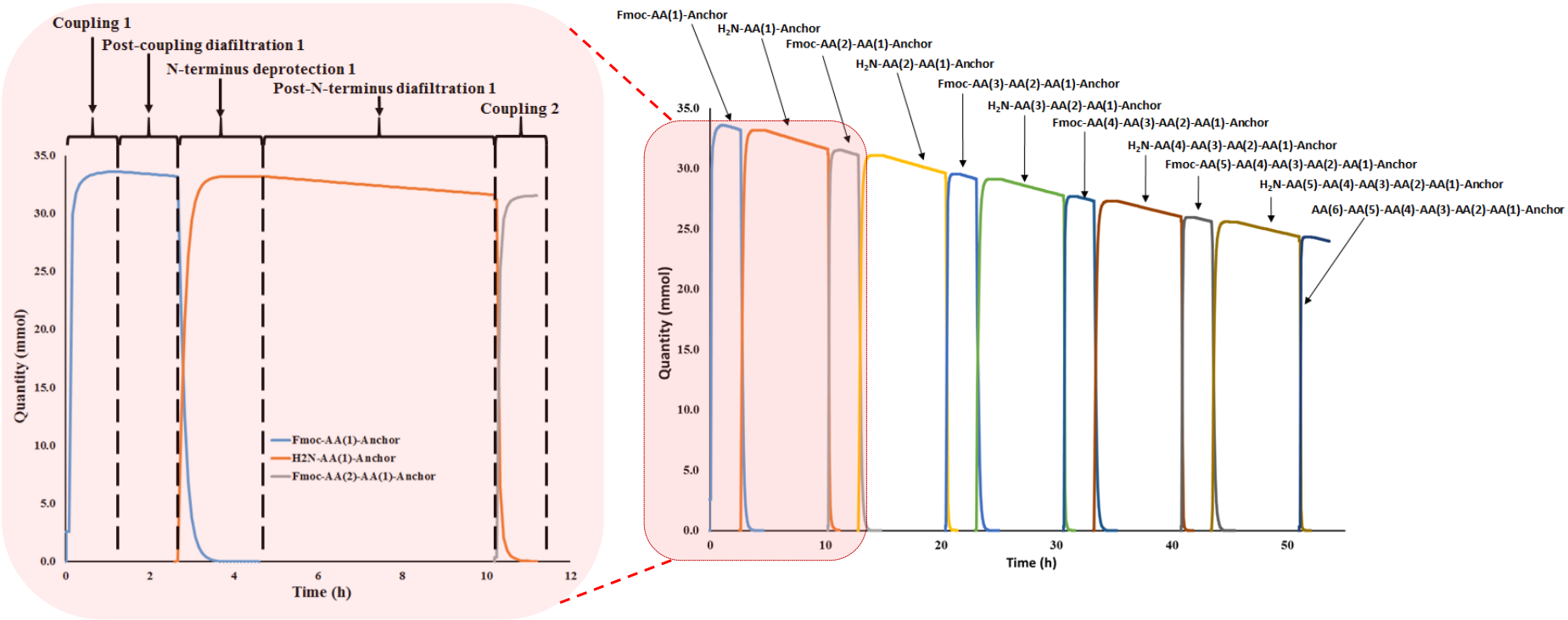

Figure 6. Quantities of anchored peptides during MEPS in a single-stage membrane system.

4.2 Extension of process model to two-stage membrane cascade

The data in Table 1 provide confidence in the accuracy of the process model, which was next extended to the two-stage configuration. The simulation inputs for two-stage MEPS are summarised in Section S3 in the supplementary information. Table 2 presents the modelling results for MEPS in both single-stage and two-stage membrane systems. With the same synthesis scale (33.6 mmol), the system volume and total membrane area increase by 124% and 90% respectively from the single-stage system to the two-stage cascade due to the additional membrane circuit.

The second-stage membrane successfully recovers the anchored peptide that permeates through the first-stage membrane, improving the overall yield significantly (i.e. 32%). However, the second-stage membrane also retains part of the excess reagents such as amino acids and piperidine that permeate through the first-stage membrane. As a result, a larger diavolume is needed (i.e. 33% more) to achieve the same purity of anchored peptide before reactions, leading to a 25% increase in process time.

As shown in Figure 7, the two-stage cascade successfully reduces the yield loss during diafiltrations by recovering the anchored peptides which permeate through the first-stage membrane due to incomplete rejection. Each operation (i.e. coupling, N-terminus deprotection, post-coupling diafiltration and post-N-terminus-deprotection) had fixed operation time as indicated in Table S3 and S4 in the supplementary information. As a result of the improved overall yield, the minimum selling price of the anchored peptide is reduced by 10% (Table 2).

Table 2. Modelling results for MEPS in single-stage and two-stage membrane systems.

	Single-stage	**Two-stage**	**Changes***
Synthesis scale (mmol)	33.6	33.5	0 %
System volume (mL)	400	894	+ 124 %
Total membrane area (A_{total}) (m^2)	0.0512	0.0973	+ 90 %
Total diavolume	92	122	+ 33 %
Total process time (h)	52	65	+ 25 %
Overall yield (%)	72.2	95.3	+ 32 %
Final purity (%)	89.1	95.8	+ 8 %
Minimum selling price (Euro · g^{-1})	37	33	- 10 %

*Change with respect to MEPS in a single-stage system.

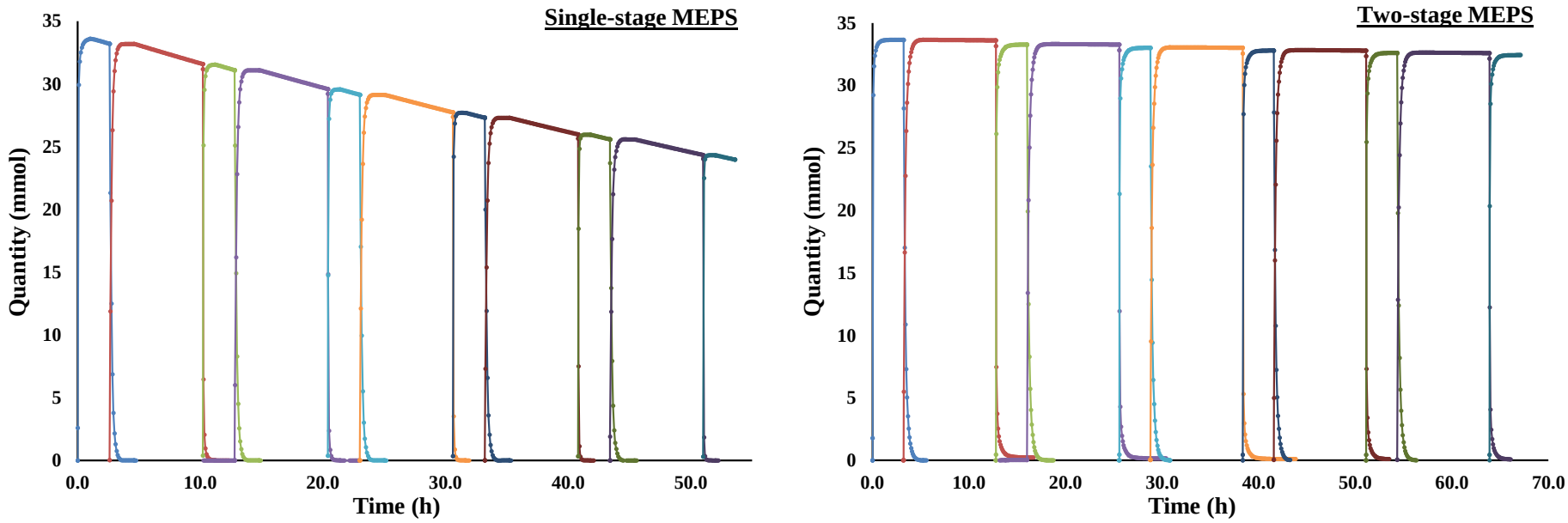

Figure 7. Quantities of anchored peptides during MEPS in single-stage and two-stage membrane systems.

4.3 Operational variable analysis

Operational variable analysis illustrates how the overall yield of anchored peptide depends on the operational variables, including the diavolumes employed for the post-coupling and post-deprotection diafiltrations, as well as the recycle ratio in the two-stage membrane cascade. The diavolume is linearly proportional to the diafiltration process time (Equation 14), whereas the recycle ratio is collectively determined by the cross-membrane pressure differences in the first- and second-stage membranes (Equation 18b). The diavolume and recycle ratio are interrelated for achieving a target purity of the anchored peptide at the end of the diafiltration process. A higher recycle ratio means more anchored peptide that permeates through the first-stage membrane as well as impurities are covered by the two-stage system, and hence a higher diavolume is required to achieve the same purity. However, the resulting yield can either increase or decrease based on the specific combination of the diavolume and recycle ratio. This means the yield and purity have a complex relationship in the case of two-stage membrane cascade, which can be studied with the current dynamic process model.

Dynamic simulations were performed, where the selected variable was perturbed while keeping all others constant. The reference value for each variable was the original input value for the simulations discussed in the previous sections. Details of the original inputs for the simulations can be found in the supplementary information. The relationships between the overall yield of anchored peptide and operational variables are different for single-stage and two-stage MEPS.

4.3.1 Sensitivity with respect to the diavolume employed for post-coupling diafiltrations

Activated amino acid is used in slight excess (0.05 equivalent) to drive each coupling to completion. At the end of each coupling, the system contains unreacted amino acid which will participate in side-reactions during the N-terminus deprotection and consumes the anchored intermediate products.

The post-coupling diafiltrations serve to remove the unreacted amino acid in the system before the N-terminus deprotection. The diavolume in two-stage MEPS is with respect to the stage 1 system volume, which includes the feed tank, pipe 1, 2 and 3, as well as the retentate compartment of the stage 1 membrane unit (Figure 5).

As the diavolume of every post-coupling diafiltration increases, the percentage of unreacted amino acid (normalised by the production scale) decreases from 5% to less than 1% for MEPS in both single-stage and two-stage membrane systems (Figure 8). However, the removal of unreacted amino acid is less efficient in the two-stage process, since the second-stage membrane not only retains the anchored intermediate product, but also the unreacted amino acid. As a result, the two-stage MEPS requires 1.4 times diavolume for post-reaction diafiltration in order to achieve the same purity level as in single-stage MEPS.

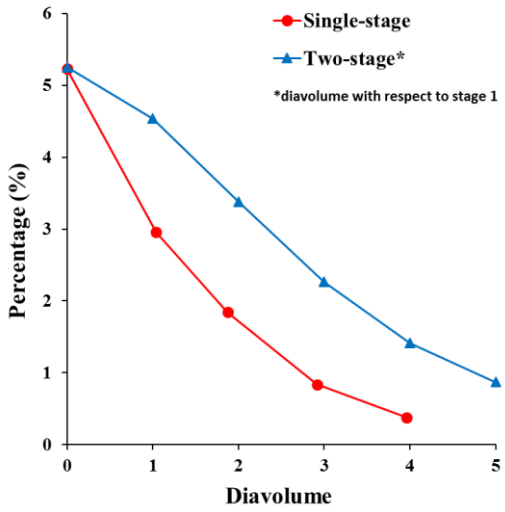

Figure 8. The quantity of unreacted amino acid at the beginning of each N-terminus-deprotection normalised by the production scale as the effect of changing the diavolume employed for every post-coupling diafiltration for single-stage and two-stage MEPS.

Although increasing the diavolume reduces the amount of unreacted amino acid in the system, and hence reduces the extent of side-reactions during the subsequent N-terminus deprotection, it also increases the loss of the anchored intermediate product through the membrane. The effect on the overall yield is therefore a combination of these two effects.

As shown in Figure 9, the overall yield decreases by 8% (i.e. from 77.6% to 72.2%) as the diavolume increases from zero to four for single-stage MEPS. This shows that the impact of the loss of anchored intermediate products during diafiltrations outweighs that of the side-reactions.

Interestingly, the effect of increasing the diavolume of every post-coupling diafiltration on the overall yield is the opposite for two-stage MEPS, as the overall yield increases slightly from 94.4% to 95.3%

(Figure 9). This is because the second-stage membrane not only retains the anchored intermediate products, but also the unreacted amino acids, which leads to a greater extent of side-reactions. A larger diavolume in two-stage MEPS reduces the quantity of unreacted amino acid in the system and therefore the extent of the resulting side-reactions.

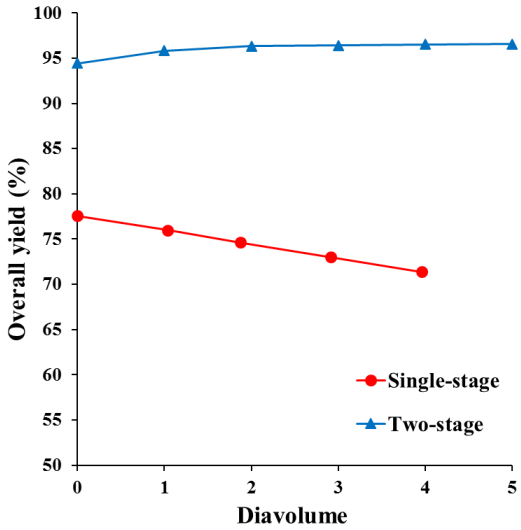

Figure 9. The effect of changing the diavolume of every post-coupling diafiltration on the overall yield for single-stage and two-stage MEPS.

4.3.2 <u>Sensitivity with respect to the diavolume employed for post-deprotection diafiltrations</u>

Piperidine is used in large excess to drive the N-terminus deprotection to completion, but it must be removed thoroughly by diafiltration before the next coupling. Otherwise, residual piperidine will consume the activated amino acid, leading to the formation of error sequences due to incomplete couplings and ultimately a lower overall yield.

Figure 10 shows that 14 diavolumes for the first post-deprotection diafiltration in the single-stage process can reduce the quantity of residual piperidine (normalised by the quantity of excess amino acid at the beginning of the following coupling) to 2.9%. Reducing this diavolume to 10 results in a higher normalised quantity of piperidine (34.9%).

Similar to the removal of excess amino acid in post-coupling diafiltration, the removal of piperidine in the two-stage process is less efficient than in its single-stage counterpart. Even with 17 diavolumes, the

normalised quantity of piperidine is relatively high (i.e. 65.6%). Decreasing the diavolume will results in a rapid increase in the normalised amount of piperidine (Figure 10).

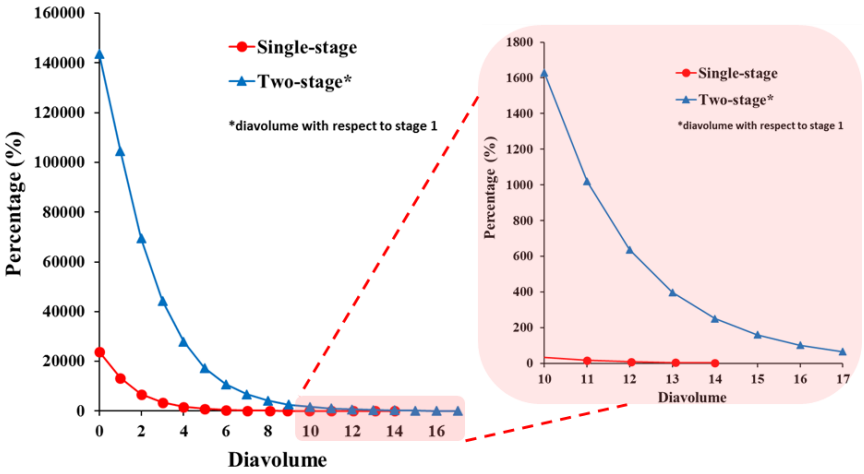

Figure 10. Quantity of residual piperidine at the end of the first post-deprotection diafiltration normalised by the quantity of excess amino acid at the beginning of the following coupling.

Figure 11 shows that the overall yield increases sharply from 0 to 7 diavolumes for single-stage MEPS and from 0 to 11 diavolumes for two-stage MEPS. These results demonstrate clearly that, unlike their post-coupling counterparts, post-deprotection diafiltrations are crucial for achieving high overall yield in both single-stage and two-stage MEPS by avoiding incomplete couplings due to the presence of residual piperidine. This result is consistent with the previous study (Chen et al., 2017).

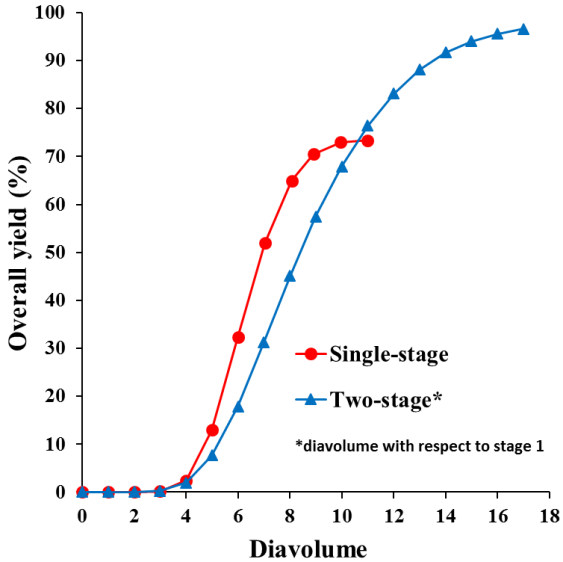

Figure 11. The effect of changing the diavolume of every post-deprotection diafiltration on the overall yield for single-stage and two-stage MEPS.

4.3.3 Sensitivity with respect to the recycle ratio in two-stage MEPS

In the two-stage process, the recycle ratio during diafiltration (Equation 18a & 18b) is another important variable that greatly influences the overall yield. It was found previously that a higher recycle ratio always results in a higher yield for the purification of polyethylene glycol 2000 (PEG 2000) from polyethylene glycol 400 (PEG 400) (Kim et al., 2013).

However, higher recycle ratio does not always result in higher overall yield for two-stage MEPS. Figure 12 shows that increasing the recycle ratio from 10% to 90% results in an initial increase in overall yield from 95.3% to 98.2% (for recycle ratio from 10% to 40%), which is followed by a slight decrease from 98.2% to 94.6%.

In other words, a recycle ratio of 40% is sufficient to improve the overall yield significantly compared to the single-stage process (i.e. from 72.2% to 98.2%). Increasing the recycle ratio further is not necessary, since this will only retain more impurities in the system and increase the diavolume required for achieving the same purity of intermediate product after each diafiltration. As mentioned in the previous sections, the increased diavolume results in lower overall yield.

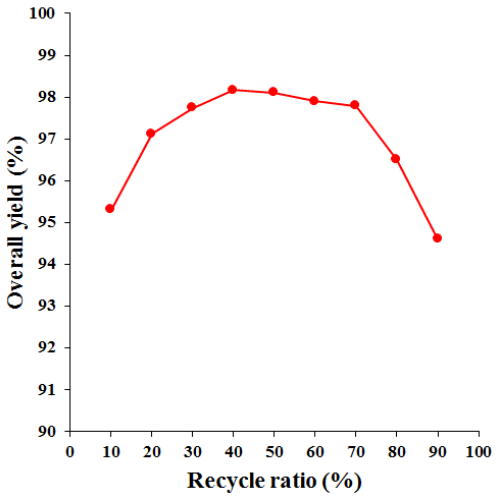

Figure 12. The effect of recycle ratio on the overall yield two-stage MEPS.

5. Conclusion

A dynamic process model was developed for the mass balance of chemical components involved in the single-stage MEPS of a model hexapeptide. The model accounts for side reactions that can happen in the presence of residual amino acid and piperidine due to their incomplete removal during diafiltrations. The process model was validated with experimental data, showing close agreement between the simulation results and the experimental results for the overall yield and purity of the anchored peptide. The extended two-stage MEPS model shows that it is indeed advantageous over single-stage MEPS, as the second-stage membrane recovers the anchored peptide that permeates through the first-stage membrane due to the incomplete retention of anchored peptide by membrane (i.e. rejection = 99.7%), leading to a significant improvement of overall yield from 72.2% to 95.3%. However, the more complex operation presented by two-stage MEPS is the trade-off for the enhanced yield, as the second-stage membrane also increases the retention of impurities (i.e. residual amino acid and piperidine) during diafiltration, resulting in more diavolumes being required (i.e. more fresh solvent and time). Operational variable analysis shows that the post-deprotection diafiltration is crucial for ensuring high overall yield. Converse to the previous study that shows a higher recycle ratio always results in higher overall yield for non-reacting systems (i.e. PEG 2000 and PEG 400), operational variable analysis shows a recycle ratio of 40% is optimal for the current two-stage MEPS, as higher recycle ratio results in higher retention of piperidine which impedes couplings. As a result, more diavolumes are required for post-deprotection diafiltrations in order to maintain a low level of residual piperidine, sacrificing the overall yield. The current dynamic model in gPROMS can be easily extended to more complex system configurations and the iterative synthesis of biopolymers in general by adapting it accordingly (the simulation file is downloadable as supplementary information of this article). For example, similar modelling and optimization frameworks can be performed for the synthesis of oligonucleotides by adding the relevant reaction rate equations into the mass balance of the model and more complex configurations such as three-stage membrane cascade can be easily constructed with an additional membrane circuit to the permeate compartment of the second-stage membrane unit.

ORCID

Wenqian Chen: 0000-0001-8867-3012

Mahdi Sharifzadeh: 0000-0002-7895-5646

Nilay Shah: 0000-0002-8906-6844

Andrew G. Livingston: 0000-0003-0074-1426

Declaration

The authors declare no competing financial interest.

Acknowledgment

Part of the current work was supported by the European Community's Seventh Framework Programme (FP7/2007-2013) [grant number 238291].

Reference

Abatemarco, T., Stickel, J., Belfort, J., Frank, B.P., Ajayan, P.M., Belfort, G., 1999. Fractionation of Multiwalled Carbon Nanotubes by Cascade Membrane Microfiltration. J. Phys. Chem. B 103, 3534–3538. https://doi.org/10.1021/jp984020n

Albericio, F., 2000. Solid-phase synthesis: a practical guide. CRC Press.

Behrendt, R., White, P., Offer, J., 2016. Advances in Fmoc solid-phase peptide synthesis. J. Pept. Sci. https://doi.org/10.1002/psc.2836

Buabeng-Baidoo, E., Majozi, T., 2015. Effective Synthesis and Optimization Framework for Integrated Water and Membrane Networks: A Focus on Reverse Osmosis Membranes. Ind. Eng. Chem. Res. 150915083245002. https://doi.org/10.1021/acs.iecr.5b01803

Castro, V., Noti, C., Chen, W., Cristau, M., Livignston, A., Rodriguez, H., Albericio, F., 2017. Novel Globular Polymeric Supports for Membrane-Enhanced Peptide Synthesis. Macromolecules 50, 1626–1634.

Caus, A., Vanderhaegen, S., Braeken, L., Van der Bruggen, B., 2009. Integrated nanofiltration cascades with low salt rejection for complete removal of pesticides in drinking water production. Desalination 241, 111–117. https://doi.org/10.1016/j.desal.2008.01.061

Cheang, B., Zydney, A.L., 2004. A two-stage ultrafiltration process for fractionation of whey protein

isolate. J. Memb. Sci. 231, 159–167. https://doi.org/10.1016/j.memsci.2003.11.014

Chen, W., 2015. Membrane Enhanced Peptide Synthesis (MEPS) – Process Development and Application. Imperial College London.

Chen, W., Sharifzadeh, M., Shah, N., Livingston, A.G., 2017. The Implication of Side-reactions in Iterative Biopolymer Synthesis: The Case of Membrane Enhanced Peptide Synthesis (MEPS). Ind. Eng. Chem. Res. 56, 6796–6804.

Coin, I., Beyermann, M., Bienert, M., 2007. Solid-phase peptide synthesis: from standard procedures to the synthesis of difficult sequences. Nat. Protoc. 2, 3247–3256. https://doi.org/10.1038/nprot.2007.454

Cseri, L., Fodi, T., Kupai, J., Balogh, G., Garforth, A., Szekely, G., 2016. Membrane-assisted catalysis in organic media. Adv. Mater. Lett.

Dong, G., Kim, J.F., Kim, J.H., Drioli, E., Lee, Y.M., 2017. Open-source predictive simulators for scale-up of direct contact membrane distillation modules for seawater desalination. Desalination 402, 72–87. https://doi.org/10.1016/j.desal.2016.08.025

Ebara, K., Ogawa, T., Takahashi, S., Nishimura, S., Kikkawa, S., Komori, S., Sawa, T., 1978. Apparatus for treating waste water or solution. 4080289.

El-Faham, A., Albericio, F., 2011. Peptide coupling reagents, more than a letter soup. Chem. Rev. https://doi.org/10.1021/cr100048w

Fikar, M., Kovács, Z., Czermak, P., 2010. Dynamic optimization of batch diafiltration processes. J. Memb. Sci. 355, 168–174. https://doi.org/10.1016/j.memsci.2010.03.019

Fodi, T., Didaskalou, C., Kupai, J., Balogh, G.T., Huszthy, P., Szekely, G., 2017. Nanofiltration-Enabled In Situ Solvent and Reagent Recycle for Sustainable Continuous-Flow Synthesis. ChemSusChem 10, 3435–3444. https://doi.org/10.1002/cssc.201701120

Gao, L., Alberto, M., Gorgojo, P., Szekely, G., Budd, P.M., 2017. High-flux PIM-1/PVDF thin film composite membranes for 1-butanol/water pervaporation. J. Memb. Sci. 529, 207–214. https://doi.org/10.1016/j.memsci.2017.02.008

Ghosh, R., 2003. Novel cascade ultrafiltration configuration for continuous, high-resolution protein-protein fractionation: A simulation study. J. Memb. Sci. 226, 85–99.

https://doi.org/10.1016/j.memsci.2003.08.012

Gravert, D.J., Janda, K.D., 1997. Organic Synthesis on Soluble Polymer Supports: Liquid-Phase Methodologies. Chem. Rev. 97, 489–510. https://doi.org/10.1021/cr960064l

Khor, C.S., Foo, D.C.Y., El-Halwagi, M.M., Tan, R.R., Shah, N., 2011. A Superstructure Optimization Approach for Membrane Separation-Based Water Regeneration Network Synthesis with Detailed Nonlinear Mechanistic Reverse Osmosis Model. Ind. Eng. Chem. Res. 50, 13444–13456. https://doi.org/10.1021/ie200665g

Kim, J.F., Freitas da Silva, A.M., Valtcheva, I.B., Livingston, A.G., 2013. When the membrane is not enough: A simplified membrane cascade using Organic Solvent Nanofiltration (OSN). Sep. Purif. Technol. 116, 277–286. https://doi.org/10.1016/j.seppur.2013.05.050

Kim, J.F., Gaffney, P.R.J., Valtcheva, I.B., Williams, G., Buswell, A.M., Anson, M.S., Livingston, A.G., 2016. Organic Solvent Nanofiltration (OSN): A New Technology Platform for Liquid-Phase Oligonucleotide Synthesis (LPOS). Org. Process Res. Dev. 20, 1439–1452. https://doi.org/10.1021/acs.oprd.6b00139

Kim, J.F., Székely, G., Valtcheva, I.B., Livingston, A.G., 2014. Increasing the sustainability of membrane processes through cascade approach and solvent recovery-pharmaceutical purification case study. Green Chem. 16, 133–145.

Li, M., 2012. Optimal plant operation of brackish water reverse osmosis (BWRO) desalination. Desalination 293, 61–68. https://doi.org/10.1016/j.desal.2012.02.024

Lightfoot, E.N., 2005. Can membrane cascades replace chromatography? Adapting binary ideal cascade theory of systems of two solutes in a single solvent. Sep. Sci. Technol. 40, 739–756.

Lutz, J.-F., Ouchi, M., Liu, D.R., Sawamoto, M., 2013. Sequence-Controlled Polymers. Science (80-.). 341, 1238149–1238149. https://doi.org/10.1126/science.1238149

Mayani, M., Mohanty, K., Filipe, C., Ghosh, R., 2009. Continuous fractionation of plasma proteins HSA and HIgG using cascade ultrafiltration systems. Sep. Purif. Technol. 70, 231–241. https://doi.org/10.1016/j.seppur.2009.10.002

Mellal, M., Hui Ding, L., Y. Jaffrin, M., Delattre, C., Michaud, P., Courtois, J., 2007. Separation and fractionation of oligouronides by shear-enhanced filtration. Sep. Sci. Technol. 42, 349–361.

Ng, P., Lundblad, J., Mitra, G., 2007. Optimization of Solute Separation by Diafiltration. Sep. Sci. 11, 499–502. https://doi.org/10.1080/01496397608085339

Overdevest, P.E.M., Hoenders, M.H.J., van't Riet, K., der Padt, A., Keurentjes, J.T.F., 2002. Enantiomer separation in a cascaded micellar-enhanced ultrafiltration system. AIChE J. 48, 1917–1926.

Rogers, M.E., Long, T.E., 2003. Synthetic Methods in Step-Growth Polymers, Synthetic Methods in Step-Growth Polymers. https://doi.org/10.1002/0471220523

Schaepertoens, M., Didaskalou, C., Kim, J.F., Livingston, A.G., Szekely, G., 2016. Solvent recycle with imperfect membranes: A semi-continuous workaround for diafiltration. J. Memb. Sci. 514, 646–658. https://doi.org/http://dx.doi.org/10.1016/j.memsci.2016.04.056

Sethi, S., Wiesner, M.R., 2000. Cost Modeling and Estimation of Crossflow Membrane Filtration Processes. Environ. Eng. Sci. 17, 61–79. https://doi.org/10.1089/ees.2000.17.61

Shi, B., Peshev, D., Marchetti, P., Zhang, S., Livingston, A.G., 2016. Multi-scale modelling of OSN batch concentration with spiral-wound membrane modules using OSN Designer. Chem. Eng. Res. Des. 109, 385–396. https://doi.org/10.1016/j.cherd.2016.02.005

So, S., Peeva, L.G., Tate, E.W., Leatherbarrow, R.J., Livingston, A.G., 2010a. Membrane enhanced peptide synthesis. Chem. Commun. 46, 2808–2810.

So, S., Peeva, L.G., Tate, E.W., Leatherbarrow, R.J., Livingston, A.G., 2010b. Organic solvent nanofiltration: A new paradigm in peptide synthesis. Org. Process Res. Dev. 14, 1313–1325. https://doi.org/10.1021/op1001403

Suárez, A., Fernández, P., Ramón Iglesias, J., Iglesias, E., Riera, F.A., 2015. Cost assessment of membrane processes: A practical example in the dairy wastewater reclamation by reverse osmosis. J. Memb. Sci. 493, 389–402. https://doi.org/10.1016/j.memsci.2015.04.065

Székely, G., Schaepertoens, M., Gaffney, P.R.J., Livingston, A.G., 2014. Beyond PEG2000: Synthesis and functionalisation of monodisperse pegylated homostars and clickable bivalent polyethyleneglycols. Chem. - A Eur. J. 20, 10038–10051. https://doi.org/10.1002/chem.201402186

van der Meer, W.G.J., Aeijelts Averink, C.W., van Dijk, J.C., 1996. Mathematical model of

nanofiltration systems. Desalination 105, 25–31. https://doi.org/10.1016/0011-9164(96)00054-9

van Reis, R., Saksena, S., 1997. Optimization diagram for membrane separations. J. Memb. Sci. 129, 19–29. https://doi.org/http://dx.doi.org/10.1016/S0376-7388(96)00319-5

Voros, N.G., Maroulis, Z.B., Marinos-Kouris, D., 1997. Short-cut structural design of reverse osmosis desalination plants. J. Memb. Sci. 127, 47–68. https://doi.org/http://dx.doi.org/10.1016/S0376-7388(96)00294-3